Desalination and Water Treatment
www.deswater.com

doi: 10.5004/dwt.2017.20253

65 (2017) 359–366
February

Evaluation of removal efficiency of fluoride from aqueous solutions using synthesis of nano-scale alumina on multi walled carbon nanotube (MWCNTs): equilibrium and kinetic studies

Hamid Zarei[a], Simin Nasseri[a], Ramin Nabizadeh Noudehi[b], Sudabeh Pourfadakari[c], Farzaneh Shemirani[d], Amir Hossein Mahvi[b,e,*]

[a]*Center for Water Quality Research, Institute for Environmental Research, Tehran University of Medical Sciences, Tehran, Iran*
[b]*School of Public Health, Tehran University of Medical Sciences, Tehran, Iran, email: ahmahvi@yahoo.com*
[c]*School of Public Health, Ahvaz Jundishapur University of Medical Sciences, Ahvaz, Iran*
[d]*Faculty of Chemical Engineering Department, Tehran University, Tehran, Iran*
[e]*Center for Solid Waste Research, Institute for Environmental Research, Tehran University of Medical Sciences, Tehran, Iran, email: ahmahvi@yahoo.com*

Received 23 March 2015; Accepted 16 October 2016

ABSTRACT

Fluoride is an essential compound in drinking water for preventing the dental caries, however excess intake of fluoride leads to various diseases. If amount of fluoride in drinking water exceeds the permissive limit, it is essential to remove fluoride from water. The aim of this study was to investigate the removal of fluoride from drinking water by nano- alumina coated on multi-walled carbon nanotubes (MWCNTs). The impact of various parameters, such as, pH, contact time, adsorbent dose, and initial fluoride concentration was investigated in the solution. The results of this research showed that, with decreasing pH from 9 to 3, removal efficiency increased, meanwhile the time for fluoride ion adsorption to reach equilibrium was 60 min. Also, increasing the adsorbent dosage from 0.5 to 1.5 g/L with fluoride concentration of 4 mg/L, resulted in increasing the removal from 70.5% to 97.1%. The results for the adsorption were fitted to the model of the Freundlich with value ($R^2 = 0.997$ at 25°C). Therefore, the combined nano- alumina/MWCNTs process was shown to be an excellent option for the removal of fluoride from drinking water.

Keywords: Adsorption; Removal of fluoride; MWCNTs; Nano- scale alumina

1. Introduction

According to World Health Organization (WHO) guidelines, the optimum fluoride level in drinking water to insure related good health is considered to be in the range of 0.5–1.5 mg/L [1]. Fluoride concentration higher than this can lead to dental and skeletal fluorosis [2]. In other words, over intake of fluoride leads to various diseases such as osteoporosis, cancer, brain damage and Alzheimer [3,4]. Fluorosis is caused by a hyper ingestion of fluoride and has caused a serious health problem for humans [5]. Depending on the fluoride concentration and the period of time of fluoride consumption in drinking water, fluoride can be beneficial or harmful for humans [6]. Fluorosis can be cause weakness of dental and skeletal structure and affect the growth, therefore, if fluoride concentration in drinking water exceeds the permissive limit, the water should be defluoridated [7]. Various physico-chemical methods have been used to remove fluoride from drinking water such as precipitation [8], ion-exchange [9], reverse osmosis [10], electrodialysis [11] and adsorption [12,13]. Chemical methods have limitation, such as complex operation, high investment, and treatment

---

* Corresponding author.

1944-3994/1944-3986

costs. Among this methods adsorption processes due to the simple design, insensitivity to toxic substances and low cost are widely used [14,15]. Various adsorbents such as, soil [16], clay [17], zeolites [18], bone char [19], activated alumina [20], granular ferric hydroxide [21] and biosorbents [22] have been successfully tested for defluoridation of drinking water. After the Long and Young reported that carbon nanotubes were more effective for removing dioxin compared with other adsorbents such as activated carbon, these materials as new adsorbents were considered [23,24]. Carbon nanotubes classified into two structures of multiwalled carbon nanotubes and singlewalled carbon nanotubes and due to having several unique physico-chemical properties such as large specific surface area, small size and cylindrical hollow structure, are very proper for pollutant removal from water and wastewater [25]. However, due to inter-particle reactions between nanotubes, dense mass is formed that reduce the surface area of the adsorbent [26]. In order to improve adsorption process and increased efficiency, the CNTs have been used with other sorbents such as; Tio_2, chitosan, and iron oxide, as support materials. Also, activated alumina compare to other inorganic oxides, due to well properties such as good capacity and selectivity, is known as one of the most substance used for fluoride removal. In this process fluoride ion can be absorbed on oxidized surface of activated alumina [27]. In this study, nano scale alumina was synthesized on multi walled carbon nanotubes (MWCNTs) as sorbent for reducing the concentration of fluoride from drinking water. In this study, the effect of different parameters on adsorption process were also investigated. In addition, the adsorption isotherms and kinetics were evaluated.

2. Materials and methods

2.1. Material

MWCNTs used in this study with over 95% purity, and a few characteristics such as specific surface area <270 m^2/g, length 10 μm, electrical conductivity 1,500 S/m and the outer diameter as 10–30 nm, were purchased from Iran's Research Institute of Petroleum Industry. SEM and TEM images of MWCNTs are shown in Figs. 1(a) and (b). The other chemicals used in this study were prepared from Merck Germany. H_2SO_4 and NaOH 1 M were used in order to adjust the pH level using a pH meter (model E520).

2.2. Synthesis of nano- alumina on MWCNTs

In order to synthesis nano- scale alumina on MWCNTs, the sol-gel chemical method was used [28]. According to this method, 1 g of MWCNTs and 37.5 g of $Al\ (NO_3)_3$ was poured into a glass container containing 50 ML of deionized water. Then, 2 ml of Triton X-100 was added as surfactant, mix and stirred for 2 h. While the mixture was stirring, sufficient amount of solid ammonium carbonate $[(NH_4)_2CO_3]$ was added to proceed complete precipitation. Then, the mixture was stirred for 1 hour at temperature 100°C and it was remained for 3 d to complete precipitation. The mixture then was filtered by a filter paper and the residue was dried for 24 h at temperature 60°C. The obtained solid material was poured in a container and then was transferred to a flask. Approximately, 25 ml of n-butanol was added into the container and sonication was done for 45 min in order to dissolve the solid. Then the solution was refluxed for 1 hour in order to removing n-butanol. The solid material obtained was transferred into a glass crucible and it was heated at temperature 800°C in argon atmosphere for 1 hour.

2.3. The characteristics of method

The size and morphology of the synthesized composite was obtained using scanning electron microscope (SEM model EM3200 Germany). Also, the crystal phases of the synthesized adsorbent was determined by X-ray diffraction (XRD). The experimental conditions of XRD measurement were as follows: Cu K_α radiation; scanning range (2θ): 10°–109°, scanning speed 5°/min, tube voltage/current, 40 kV/30 mA.

2.4. Adsorption experiments

The experiments were carried out in a batch systems at temperature (25°C). The stock solution (100 mg/L) was prepared by dissolving 0.221 g NaF (analytical grade) in 1 L of deionized water. All fluoride solutions were prepared by diluting the stock solution in appropriate proportions, and the experiments were conducted in 100 mL glass flasks. The effect of various parameters, including reaction time (10–120 min), initial fluoride concentration (2, 4, 6 and 8 mg/L), pH (3–9) and adsorbent concentration (0.25, 0.5, 1 and 1.5 g/L) on the fluoride removal process were assessed.

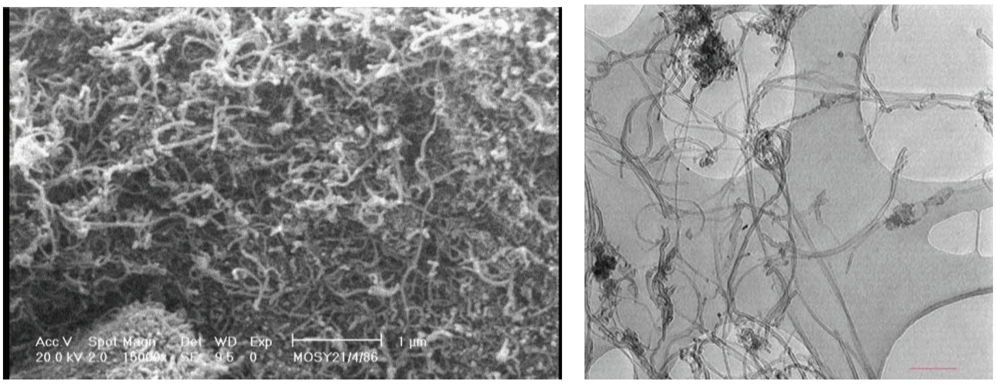

Fig. 1. (a) SEM and (b) TEM of a (MWCNTs).

The experiments was done using a shaker (models Heidol pH) at a constant speed of 220 rpm in order to mix samples with adsorbent at the end of equilibrium time. To separate the adsorbent from the fluoride solution, the samples were centrifuged at 4,000 rpm for 5 min and passed from 0.45 µ filter paper and the concentration of residual fluoride was measured by spectrophotometer UV/Vis (Hatch – DR2000, Germany) at the wavelength of 580 nm according to the standard methods [29]. The amount of fluoride adsorbed by the adsorbent (mg/g) and adsorption efficiency (%) were obtained using Eqs. (1) and (2) [30].

$$q_e = \frac{\left(C_0 - C_t\right)V}{M} \tag{1}$$

$$\mathrm{Re}\left(\%\right) = \frac{\left(C_0 - C_t\right)}{C_0} \times 100 \tag{2}$$

where C_0 and C_t are the initial fluoride concentration and the remaining fluoride concentration in the solution (mg/L), q_e is the amount of adsorbed fluoride (mg/g), V is the volume (L) and M is the adsorption mass expressed (g) and R is the efficiency of removal. Also, In order to further understand the characteristics of the adsorption process, the isotherm model and the kinetic model were investigated.

2.5. Determination of point of zero charge (pzc)

Point of zero charge (pzc) value was determined using solid addition method [31]. According to this method, two similar solutions (blank and sample) were prepared. 40 mL of KCl and fluoride solutions were poured to a series of 50 mL glass tubes. The pH of the solutions was adjusted in the range of 2.0–12.0 by adding HCl and NaOH 0.1 M. The total volume of the solution in each tube was adjusted exactly to 50 mL by adding KCl and fluoride solution. Then, 0.5 g of sorbent was added to all tubes and the suspension was shaken for 48 h to reach equilibration. After this time, the solutions were filtered and pH value was measured. The difference between the initial and final pH values ($\mathrm{pH} = \mathrm{pH}_i – \mathrm{pH}_f$) was plotted. The $\mathrm{pH}_{\mathrm{ZPC}}$ was taken as the point which the net electric charge of the adsorbent surface is zero. It was evident that at pHi = 6.5, ΔpH was zero. Therefore the $\mathrm{pH}_{\mathrm{ZPC}}$ was estimated at 6.5.

3. Results and discussion

3.1. Characterization of alumina nanoparticles on MWCNTs

SEM and XRD images of the synthesized composite are presented in Figs. 2 and 3. As in the SEM images shown, the morphology of two surfaces in blank MWCNTs, Fig. 1(a) and synthesized composite in Fig. 2, were different. Also, it was observed that aluminum oxide nanoparticles were successfully deposited on the surface of MWCNTs, and the average alumina nanoparticle/MWCNTs size was below 53 nm. According to Fig. 3 in the XRD patterns of MWCNTs/alumina nanoparticle composite, the diffraction peaks of alumina nanoparticle on MWCNTs can be observed. The main dominant peaks were identified at 2θ = 28°, 39°, 43° and 78°, which related to existence of crystalline phases in nano-scale alumina on MWCNTs.

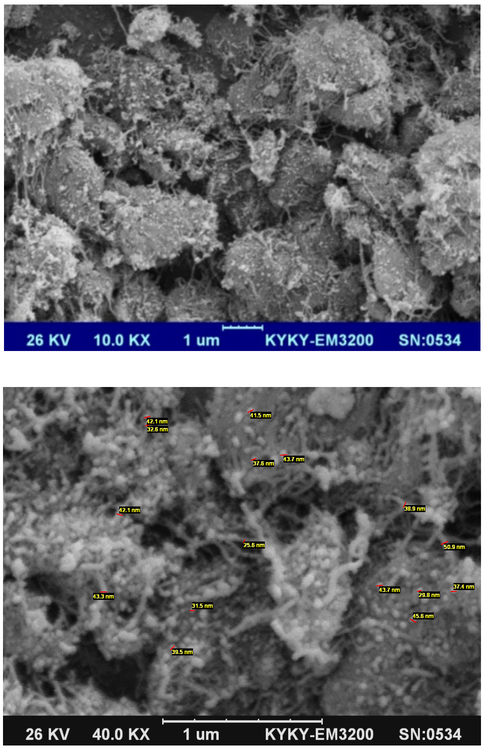

Fig. 2. SEM photograph of alumina nanoparticle on MWCNTs from a different angle.

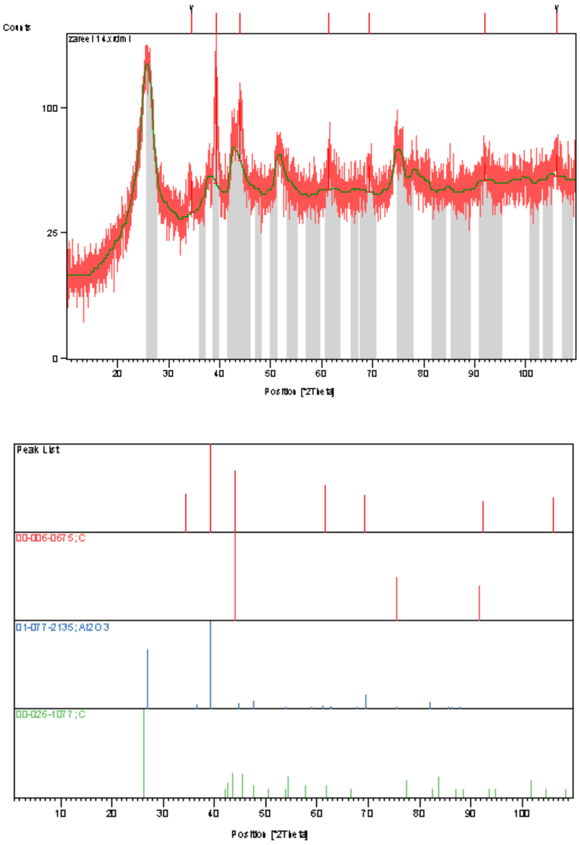

Fig. 3. XRD pattern of the alumina nanoparticle/MWCNTs.

3.2. The effect of contact time

The effect of contact time (10–120 min) in removal of fluoride by alumina nanoparticle/MWCNTs from drinking water was investigated with adsorbent dose of 0.5 gr, PH = 3 and different concentration of fluoride (2, 4, 6, 8 mg/L) at room temperature. According to the obtained results in Fig. 4, with increasing time in the first 45 min, with concentration of 2 mg/L of fluoride, removal efficiency increased to more than 96.5% and after this time, the adsorption amount increased with a mild slope until reached equilibrium after 60 min. Also, by increasing the contact time from 10 to 45, the adsorption capacity increased from 3.44 to 3.86 mg/g and the maximum adsorption capacity was obtained as 3.9 mg/g at 60 min. This might be, because, during the early stages of the process there are a large number of empty sites on adsorbent surface, and with passing of time, this spaces are occupied by fluoride ions [32]. In a study conducted by Sujana and Mohanty [33] on fluoride uptake using nano-scale iron oxide-hydroxide, the results obtained showed that, the removal efficiency during 30 min reached to 90% and then followed a steady slope and reached equilibrium after 1 h. by increasing the contact time, the dye adsorption capacity increased with a sharp manner and the adsorption capacity increased from 91.63 to 127.233 mg/g.

3.3. The effect of the initial fluoride concentration

The effect of different fluoride concentration on the removal was evaluated and the results are shown in Fig. 5. According to the results, with increasing fluoride concentration from 2 to 8 mg/L at the adsorbent dose of 0.5 g/L, PH = 3, and equilibrium time, the removal percentages of fluoride decreased from 97.21% to 72.3%. This reason is probably because of this fact that, at the low concentration, the large number of empty sites on the adsorbent surface are available, and with increasing concentration of adsorbate, these spaces are occupied [34].

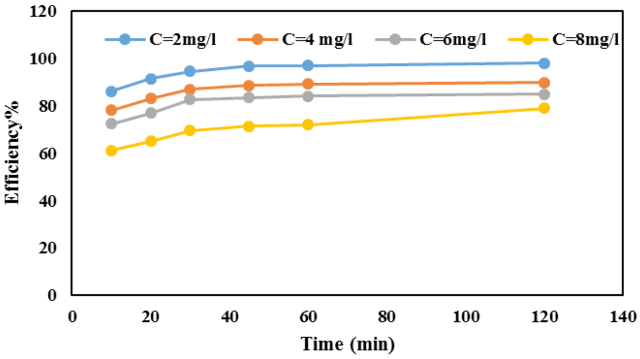

Fig. 4. The effect of contact time on fluoride adsorption by alumina nanoparticle/MWCNTs (adsorbent dose = 0.5 g/L, pH = 3).

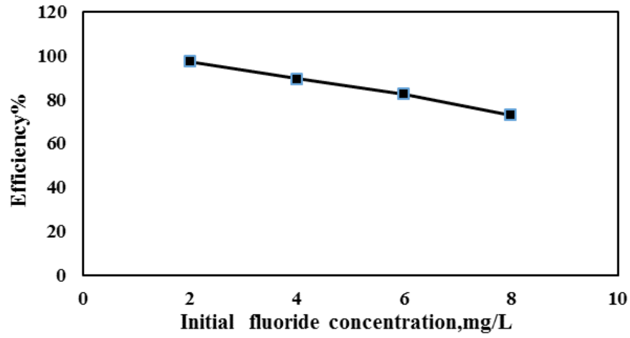

Fig. 5. Effect of initial concentration on fluoride adsorption by alumina nanoparticle/MWCNTs (adsorbent dose = 0.5 g/L, pH = 3).

3.4. Effect of pH

In order to assess the effect of pH on fluoride removal, the experiments were performed at the pH range of 3–9, adsorbent dose of 0.5 g/L, and different fluoride concentration at equilibrium time and room temperature. It is evident from Fig. 6, that by reducing pH, removal efficiency increases. The best adsorption of fluoride occurred at pH 3.0 (lower than PHzpc), because at pH lower than pHzpc, the surface charges were positive, favoring anion adsorption. This occurs due to the fact that the functional oxygen groups on the surface of nanoparticles play an important role, and in acidic pH concentration of $H^{+\ ion}$ increased and lead to increased bonding between H^+ groups on the surface of nanoparticles and decrease in the OH-, and increase in the positive ions on the surface of the adsorbent. Also, this process will lead to increase the electrostatic force between the fluoride molecules (negatively charged) and the surface of the adsorbent (positively charged), and increase the adsorption capacity [35]. In study conducted by Mahramanlioglu et al. on removal fluoride with acid treated spent bleaching, the obtained results showed that in pH = 3.5, the maximum removal efficiency reached to 49% [36].

3.5. Effect of adsorbent dosage

The effect of adsorbent dosage on the adsorption process was studied at pH = 3, contact time of 60 min and different fluoride concentration, the results are shown in Fig. 7. According to this results, with increase in adsorbent dose from 0.25 to 1.5 g/L, in initial fluoride concentration of 4 mg/L, the percentage of fluoride removal increased from 70.5% to 97.09% and the optimum dose of adsorbent was 1.5 g/L. The probable reason related to this subject is that with increase in the adsorbent dose, the more activated adsorption

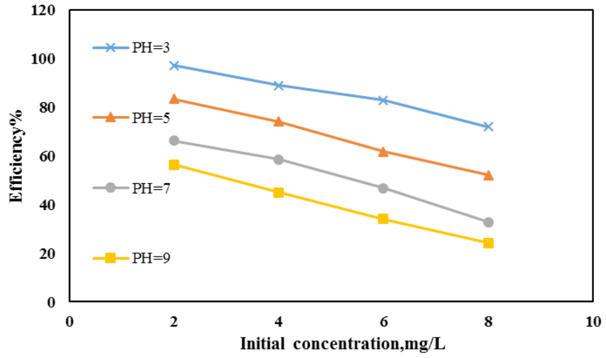

Fig. 6. Effect of pH on fluoride sorption by alumina nanoparticle/MWCNTs (sorbent dose = 0.5 g L^{-1}; contact time = 60 min and different fluoride concentration).

sites will be available and the specific surface area will be extended [37]. Daifullah et al. studied fluoride removal with $KMnO_4$-modified activated carbon, the results showed that by increasing carbon dose, removal percent raised [38].

3.6. Adsorption isotherm

The relation between the adsorbate and adsorbent in solution can be expressed by adsorption isotherm, in this study Langmuir, Freundlich and Temkin isotherm models was used to describe the equilibrium behavior of adsorption process. The experiments were performed by adding the adsorbent dose of 1 g/L to different fluoride concentration at pH = 3, the equilibrium time and temperature of 25°C. The assumption of the Langmuir isotherm model is homogenous surface energy distribution. Also, The Freundlich isotherm describes equilibrium on heterogeneous surfaces and hence does not assume monolayer capacity. The equations and linear forms of these isotherms presented as follows [39]:

A, Langmuir isotherm model is as follows:

$$q_e = \frac{Q_m K_L C_e}{1 + K_L C_e} \tag{3}$$

$$\frac{1}{q_e} = \frac{1}{Q_m} + \left(\frac{1}{K_L Q_m}\right)\frac{1}{C_e} \tag{4}$$

where q_e, is the amount of adsorbed fluoride (mg/gr), $C_{e,}$ is the equilibrium concentration of adsorbate (mg/L), $K_{L,}$ is the Langmuir constant (L/mg), $Q_{m,}$ is a maximum adsorption capacity of the fluoride (mg/g) per unit weight of adsorbent.

B, Ferundlich isotherm equation is as follows:

$$q_e = K_f C_e^{\frac{1}{n}} \tag{5}$$

The linear form of the Ferundlich equation is also presented as follows:

$$\log q_e = \log K_f + \left(\frac{1}{n}\right)\log C_e \tag{6}$$

where q_e, is the amount of adsorbed fluoride per unit mass of the adsorbent (mg/gr), C_e, is adsorbate concentration in the solution at equilibrium (mg/L), K_f and n, are constants indicating adsorption capacity and intensity, respectively.

C, Temkin isotherm equation and linear form is as follows:

$$q_e = B_1 Ln(k_T C_e) \tag{7}$$

$$q_e = B_1 \ln k_T + B_1 \ln C_e \tag{8}$$

K_T and B_1 = RT/b are Temkin isotherm constant, R, is the universal gas constant (8.314 j/mol k), T, is the temperature at (°k), K_t is the equilibrium bond constant (L/g), and $B_{1,}$ is related to the adsorption heat.

The results related to these isotherms are shown in Fig. 8 and Table 1. According to the obtained results, it can be seen that the experimental data were better fitted by Ferundlich isotherm model (R^2 = 0.997), the value of n = 2.48, at 25°C was greater than 1, which indicates the favorable removal conditions. Also, the adsorption of fluoride on nano alumina/MWCNTs is physical, and this is related to large surface area of alumina nanoparticle/MWCNTs, but low maximum fluoride adsorption capacity. In study conducted by Tor et al. on

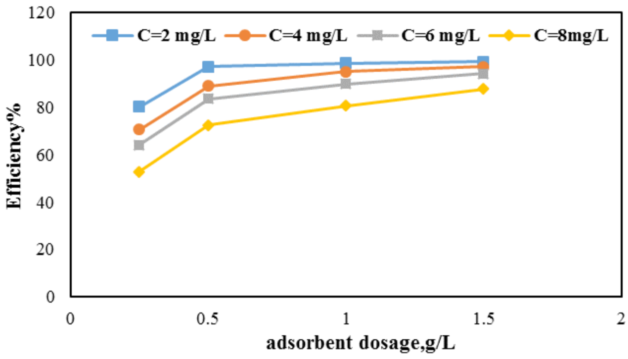

Fig. 7. Effect of adsorbent dose on fluoride sorption by alumina nanoparticle/MWCNTs (pH = 3 dose = 0.5 g/L, contact time = 60 min and different fluoride concentration).

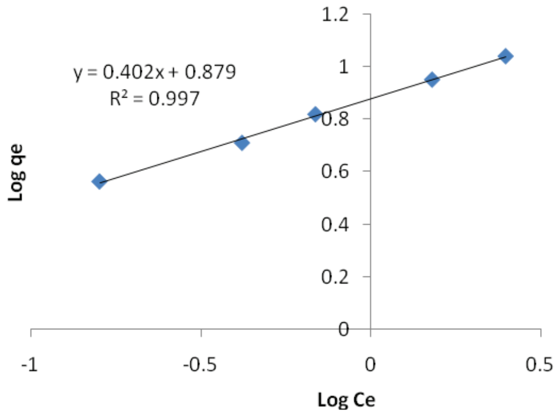

Fig. 8. Modeling the Freundlich adsorption isotherm for fluoride adsorption using alumina nanoparticle/MWCNTs.

Table 1
The results of computation of the study adsorption isotherm

Type of isotherm	Isotherm parameters	Temperature (°C)
		25
Freundlich	n	2.48
	K_f	7.56
	R^2	0.997
Langmuir	Q_m	13.15
	K_1	1.172
	R^2	0.981
Temkin	K_T	2.065
	B_T	1199
	R^2	0.980

Table 2
Defluoridation of water sample by different methods

Adsorbent	Amount adsorbed (mg/g)	Experimental conditions	References
Granular activated alumina (PURALOX)	2.232	Concentration: 10 mg/L	[41]
Copper oxide coated alumina	7.220	Temperature: 30°C ± 1°C	
Iron(III)–Tin(IV) mixed oxide	10.47	pH: 6.4 Concentration: 10–50 mg/L Temperature: 303 K	[42]
Fe–Al–Ce nano-adsorbent	2.22	pH: 7.0 Concentration: 0.0001 M Temperature: 25°C	[43]
Scandinavia spruce wood charcoal (AlFe650/C)	13.64	pH: 7.0 Temperature: 28°C ± 2°C Concentration: 2–50 mg/L	[44]
Chemical treated laterite	37.9	pH: 5.0 Concentration: 3–50 mg/L Temperature: 305 K	[45]
Magnetic-chitosan	22.49	pH: 7.0 Concentration: 5–140 mg/L	[46]
Hydrous-manganese-oxide-coated alumina	7.09	pH: 5.2 Concentration: 10–70 mg/L Temperature: 30°C	[47]
Hydrotalcite/chitosan composite	1.255	Temperature: 30°C Concentration: up to 15 mg/L pH: acidic pH	[48]
Granular ceramic	12.12	Temperature: 20°C Concentration: 5–50 mg/L pH: 6.90	[49]
Nano-alumina	14.0	pH: 6.15 Concentration: 1–100 mg/L Temperature: 25°C	[50]
Nano-scale alumina on multi walled carbon nanotubes	13.15	pH: 3 Concentration: 2–8 mg/L Temperature: 25°C	Present work

removal of fluoride by using montmorillonite, the obtained results showed that Freundlich isotherm was the best model for adsorption reaction [40]. Also, the maximum adsorption capacity of fluoride and experimental conditions in the present study was compared with other articles and results are summarized in Table 2.

3.7. Kinetic studies

In order to investigate the characteristics adsorption process of fluoride on alumina nanoparticle/MWCNTs, kinetic studies were performed using pseudo-first-order, pseudo-second-order and Intraparticle diffusion models that most generally used to describe the adsorption process. Kinetic equations and linear forms used in this study are the following [51]:

A: pseudo-first-order model:

$$\frac{dq_t}{dt} = k_1(q_e - q_t) \tag{9}$$

$$\log(q_e - q_t) = \log(q_e) - \frac{k_1}{2.303}t \tag{10}$$

where q_t (mg/g) is the amount adsorption of adsorbate on the adsorbent at time t (min); q_e (mg/g) is the adsorption capacity at equilibrium time; and k_1 (min^{-1}) is the equilibrium rate constant and t is the contact time (min). The value of k_1 was calculated from the slope of the linear plot of log (q_e–q) vs. time

B: pseudo-second-order model:

$$\frac{dq_t}{dt} = k_2(q_e - q_t)^2 \tag{11}$$

$$\frac{t}{q_t} = \left(\frac{1}{k_2 q_e^2}\right) + \left(\frac{1}{q_e}\right)t \tag{12}$$

where k_2 (g/mg min) is the rate constants for the pseudo-second-order model.

Table 3
The results of studying the kinetics

Kinetics of	Parameter kinetics	Concentration mg/L			
		2	4	6	8
Pseudo-first-order	K_1	0.062	0.041	0.05	0.046
	q_{ecal}	4.77	1.67	1.19	2.6
	R^2	0.99	0.97	0.97	0.97
Pseudo-second-order	K_2	0.52	0.097	0.094	0.018
	q_{ecal}	1.91	3.84	5.43	7.4
	R^2	1	0.999	0.999	0.998
Intraparticle diffusion	K_{dif}	0.01	0.06	0.07	0.26
	C	1.74	3.084	4.57	4.27
	R^2	0.84	0.94	0.89	0.96

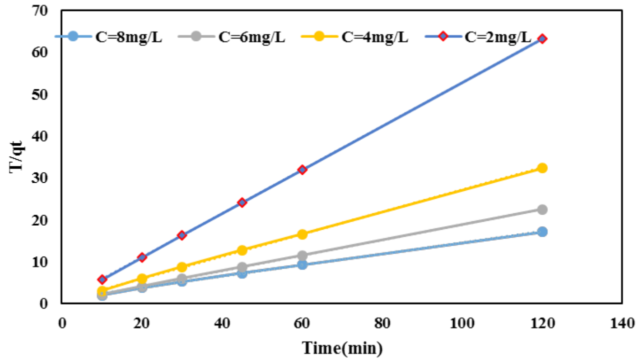

Fig. 9. Modeling the pseudo-second-order kinetic for fluoride adsorption using alumina nanoparticle/MWCNTs.

C: Intraparticle diffusion.

$$q_t = K_{dif} t^{0.5} + C \tag{13}$$

where C is the intercept and k_{dif} indicates the intraparticle diffusion rate constant (mg/g min $^{0.5}$).

The results and parameters of the Kinetic equations and their correlation coefficients are shown in Table 3 and Fig. 9. As seen in Table 3, the correlation coefficients of the pseudo-second-order kinetic model with (R^2) = 0.999, is more appropriate to describe the adsorption behavior of fluoride on alumina nanoparticle/MWCNTs compared with pseudo-first-order model. These results are similar with the results from Maliyekkal et al. about removal of fluoride with manganese-oxide-coated alumina [52].

4. Conclusions

The obtained results from the present study demonstrated that acidic pH is one of the effective factors in increasing the efficiency of nano- alumina/MWCNTs, and the maximum fluoride uptake capacity was observed at pH = 3. However, the maximum absorption was observed at contact time = 60 min and 1.5 g/L dose of adsorbent. Also, pseudo-second-order kinetic model and Freundlich isotherm are much fit better for describing adsorption process of fluoride from water sample using nano- alumina/MWCNTs.

Acknowledgments

This study was part of a thesis that financially was supported by Center for Water Quality Research, Institute for Environmental Research, Tehran University of Medical Sciences. The authors would like to thank the laboratory staff of School of Public Health.

References

[1] D.P. Das, J. Das, K. Parida, Physicochemical characterization and adsorption behavior of calcined Zn/Al hydrotalcite-like compound (HTlc) towards removal of fluoride from aqueous solution, J. Colloid Interface Sci., 261 (2003) 213–220.
[2] P. Bagheri Ardabilian, M. Mosaferi, A. Sharifyan, Removal of fluoride from water using an alumina modified with iron compounds, J. Civil Environ. Eng., 43 (2014) 1–3.
[3] N. Chinoy, Effects of fluoride on physiology of animals and human beings, Indian J. Environ. Toxicol., 1 (1991) 17–32.
[4] P.T. Harrison, Fluoride in water: a UK perspective, J. Fluorine Chem., 126 (2005) 1448–1456.
[5] X. Fan, D. Parker, M. Smith, Adsorption kinetics of fluoride on low cost materials, Water Res., 37 (2003) 4929–4937.
[6] M. Mahramanlioglu, I. Kizilcikli, I. Bicer, Adsorption of fluoride from aqueous solution by acid treated spent bleaching earth, J. Fluorine Chem., 115 (2002) 41–47.
[7] M.R. Boldaji, A.H. Mahvi, S. Dobaradaran, S.S. Hosseini, Evaluating the effectiveness of a hybrid sorbent resin in removing fluoride from water, Int. J. Environ. Sci. Technol., 6 (2009) 629–632.
[8] S. Saha, Treatment of aqueous effluent for fluoride removal, Water Res., 27 (1993) 1347–1350.
[9] K.Vaaramaa, J. Lehto, Removal of metals and anions from drinking water by ion exchange, Desalination, 155 (2003) 157–170.
[10] P.I. Ndiaye, P. Moulin, L. Dominguez, J.C. Millet, F. Charbit, Removal of fluoride from electronic industrial effluentby RO membrane separation, Desalination, 173 (2005) 25–32.
[11] Z. Amor, B. Bariou, N. Mameri, M. Taky, S. Nicolas, Fluoride removal from brackish water by electrodialysis, Desalination, 133 (2001) 215–223.
[12] S. Ghorai, K. Pant, Investigations on the column performance of fluoride adsorption by activated alumina in a fixed-bed, J. Chem. Eng., 98 (2004) 165–173.
[13] A. Daifullah, S. Yakout, S. Elreefy, Adsorption of fluoride in aqueous solutions using $KMnO_4$-modified activated carbon derived from steam pyrolysis of rice straw, J. Hazard. Mater., 147 (2007) 633–643.
[14] A. Maleki, A.H. Mahvi, M.A. Zazouli, H. Izanloo, A.H. Barati, Aqueous cadmium removal by adsorption on barley hull and barley hull ash, Asian J. Chem., 23 (2011) 1373–1376.
[15] A.H. Mahvi, F. Gholami, S. Nazmara, Cadmium biosorption from wastewater by Ulmus leaves and their ash, Eur. J. Sci. Res., 23 (2008) 197–203.
[16] Y. Wang, E.J. Reardon, Activation and regeneration of a soil sorbent for defluoridation of drinking water, Appl. Geochem., 16 (2001) 531–539.
[17] G. Moges, F. Zewge, M. Socher, Preliminary investigations on the defluoridation of water using fired clay chips, J. Afr. Earth Sci., 22 (1996) 479–482.
[18] M.S. Onyango, Y. Kojima, A. Kumar, D. Kuchar, M. Kubota, Uptake of fluoride by $Al3^+$ pretreated low-silica synthetic zeolites: adsorption equilibrium and rate studies, Separ. Sci. Technol., 41 (2006) 683–704.
[19] D. Bhargava, D. Killedar, Fluoride adsorption on fishbone charcoal through a moving media adsorber, Water Res., 26 (1992) 781–788.
[20] S. Ghorai, K.K. Pant, Equilibrium, kinetics and breakthrough studies for adsorption of fluoride on activated alumina, Separ. Purif. Technol., 42 (2005) 265–271.
[21] E. Kumar, A. Bhatnagar, M. Ji, W. Jung, S.H. Lee, S.J. Kim, Defluoridation from aqueous solutions by granular ferric hydroxide (GFH), Water Res., 43 (2009) 490–498.

[22] S. Venkata Mohan, S.V. Ramanaiah, B. Rajkumar, P.N. Sarma, Removal of fluoride from aqueous phase by biosorption onto algal biosorbent *Spirogyra* sp.-IO_2: sorption mechanism elucidation, J. Hazard. Mater., 141 (2007) 465–474.

[23] M. Shirmardi, A. Mesdaghinia, A.H. Mahvi, S. Nasseri, R. Nabizadeh, Kinetics and equilibrium studies on adsorption of acid red 18 (azo-dye) using multiwall carbon nanotubes (MWCNTs) from aqueous solution, E-J. Chem., 9 (2012) 2371–2383.

[24] M.A. Baghapour, S. Pourfadakari, A.H. Mahvi, Investigation of reactive red dye 198 removal using multiwall carbon nanotubes in aqueous solution, J. Ind. Eng. Chem., 20 (2014) 2921–2926.

[25] M.A. Baghapour, A.H. Mahvi, S. Pourfadakari, Thermodynamic analysis of Reactive Red 198 removal from synthetic wastewater by using multiwall carbon nanotubes, J. Health Scope, 2 (2013) 149–155.

[26] G.A. Haghighat, M.H. Dehghani, S. Nasseri, A.H. Mahvi, N. Rastkari, Comparison of carbon nonotubes and activated alumina efficiencies in fluoride removal from drinking water, Indian J. Sci. Technol., 5 (2012) 2432–2435.

[27] Y.H. Li, S. Wang, A. Cao, D. Zhao, et al., Adsorption of fluoride from water by amorphous alumina supported on carbon nanotubes, Chem. Phys. Lett., 350 (2001) 412–416.

[28] F. Mirjalili, M. Hasmaliza, L. Chuah, Abdullah, Size-controlled synthesis of nano a-alumina particles through the sol–gel method, Ceramics Int., 36 (2010) 1253–1257.

[29] L. Clesceri, A. Greenberg, A. Eaton, Standard Methods for the Examination of Water and Wastewater, APHA, AWWA, WEF, USA, 20 Ed., 2010.

[30] A.H. Mahvi, M.A. Zazoli, M. Younecian, B. Nicpour, A. Babapour, Survey of fluoride concentration in drinking water sources and prevalence of DMFT in the 12 years old students in Behshar city, J. Med. Sci., 6 (2006) 658–661.

[31] D.H. Lataye, I.M. Mishra, I.D. Mall, Removal of pyridine from aqueous solution by adsorption on bagasse fly ash, Ind. Eng. Chem. Res., 45 (2006) 3934–3943.

[32] M. Ansari, M. Kazemipour, M. Dehghani, M. Kazemipour, The defluoridation of drinking water using multi-walled carbon nanotubes, J. Fluorine Chem., 132 (2011) 516–520.

[33] M.G. Sujana, S. Mohanty, Characterization and fluoride uptake studies of nano-scale iron oxide-hydroxide synthesized by microemulsion method, Int. J. Eng. Sci. Technol., 2 (2010) 1–12.

[34] M. Poudyal, S. Babel, Removal of fluoride using granular activated carbon and domestic sewage sludge, Int. Conf. Inform. Environ. Energy Appl., 89 (2015) 139–143.

[35] F. Shen, X. Chen, P. Gao, G. Chen, Electrochemical removal of fluoride ions from industrial wastewater, J. Chem. Eng. Sci., 58 (2003) 987–993.

[36] M. Mahramanlioglu, I. Kizilcikli, I.O. Bicer, Adsorption of fluoride from aqueous solution by acid treated spent bleaching earth, J. Fluorine Chem., 115 (2002) 41–47.

[37] H.S. Jahin, Fluoride removal from water using nanoscale zero-valent iron, Int. J. Water Technol., 4 (2014) 172–182.

[38] A.A.M. Daifullah, S.M. Yakout, S.A. Elreefy, Adsorption of fluoride in aqueous solutions using $KMnO_4$-modified activated carbon derived from steam pyrolysis of rice straw, J. Hazard Mater., 147 (2007) 633–643.

[39] A.O. Dada, A.P. Olalekan, A.M. Olatunya, O. Dada, Langmuir, Freundlich, Temkin and Dubinin–Radushkevich isotherms studies of equilibrium sorption of Zn^{2+} unto phosphoric acid modified rice husk, IOSR J. Appl. Chem., 3 (2012) 38–45.

[40] A. Tor, Removal of fluoride from an aqueous solution by using montmorillonite, Desalination, 201 (2006) 267–276.

[41] A. Bansiwal, P. Pillewan, R.B. Biniwale, S.S. Rayalu, Copper oxide incorporated mesoporous alumina for defluoridation of drinking water, Microporous Mesoporous Mater., 129 (2010) 54–61.

[42] K. Biswas, K. Gupta, U.C. Ghosh, Adsorption of fluoride by hydrous iron (III)–tin (IV) bimetal mixed oxide from the aqueous solutions, J. Chem. Eng., 149 (2009) 196–206.

[43] L. Chen, H.X. Wu, T.J. Wang, Y. Jin, Y. Zhang, X.M. Dou, Granulation of Fe–Al–Ce nano-adsorbent for fluoride removal from drinking water by spray coating on sand in a fluidized bed, J. Powder Technol., 193 (2009) 59–64.

[44] E. Tchomgui-Kamga, V. Alonzo, Ch.P. Nanseu-Njiki, N. Audebrand, E. Ngameni, A. Darchen, Preparation and characterization of charcoals that contain dispersed aluminum oxide as adsorbents for removal of fluoride from drinking water, Carbon, 48 (2010) 333–343.

[45] A. Maiti, J.K. Basu, S. De, Chemical treated laterite as promising fluoride adsorbent for aqueous system and kinetic modeling, Desalination, 265 (2011) 28–36.

[46] W. Ma, F.Q. Ya, M. Han, R. Wang, Characteristics of equilibrium, kinetics studies for adsorption of fluoride on magnetic-chitosan particle, J. Hazard. Mater., 143 (2007) 296–302.

[47] S.X. Teng, S.G. Wang, W.X. Gong, X.W. Liu, Removal of fluoride by hydrous manganese oxide-coated alumina: performance and mechanism, J. Hazard. Mater., 168 (2009) 1004–1011.

[48] N. Viswanathan, S. Meenakshi, Selective fluoride adsorption by a hydrotalcite/chitosan composite, Appl. Clay Sci., 48 (2010) 607–611.

[49] N. Chen, Z. Zhang, C. Feng, N. Sugiura, M. Li, Fluoride removal from water by granular ceramic adsorption, J. Colloid Interface Sci., 348 (2010) 579–584.

[50] E. Kumar, A. Bhatnagar, U. Kumar, M. Sillanpää, Defluoridation from aqueous solutions by nano-alumina: characterization and sorption studies, J. Hazard. Mater.,186 (2011) 1042–1049.

[51] M.G. Sujana, S. Mohanty, Characterization and fluoride uptake studies of nano-scale iron oxide-hydroxide synthesized by microemulsion method, Int. J. Eng. Sci. Technol., 2 (2010) 1–12.

[52] S.M. Maliyekkal, A.K. Sharma, L. Philip, Manganese-oxide-coated alumina: a promising sorbent for defluoridation of water, Water Res., 40 (2006) 3497–3506.